Optics and Spectroscopy, 2024, Vol. 132, No. 8

11

On the theory of tip-enhanced Raman scattering (TERS) in two-dimensional materials

© *D.M. Basko*

Univ. Grenoble Alpes and CNRS, LPMMC,
38042 Grenoble, France

email: denis.basko@lpmmc.cnrs.fr

Received July 08, 2024
Revised July 08, 2024
Accepted July 29, 2024

We consider tip-enhanced Raman scattering (TERS) on phonons in two-dimensional materials such as graphene or transition metal dichalcogenides. The main question addressed here is what information about phonons at non-zero wave vectors can be extracted from the dependence of the Raman spectrum on the tip position with respect to the sample. It is shown that for single-phonon non-resonant scattering the measurable quantity is the convolution of the phonon spectral function with respect to wavevector with a certain integral kernel, which is determined by the geometry and dielectric properties of the whole structure. The explicit form of this integral kernel is calculated in the simplest model, where the tip is represented by a point polarizable dipole.

Keywords: Raman scattering, TERS, spectral function.

DOI: 10.61011/EOS.2024.08.60032.6873-24

Introduction

Theoretical study of the optical properties of low-dimensional structures was started in the pioneering work by V.M. Agranovich and O.A. Dubovsky [1]. Ahead of its time by decades, this work received the deserved attention closer to the end of the 20th century when advances in nanotechnology made it possible to grow structures with predefined properties [2,3]. In the 21st century, production of two-dimensional monolayers of graphene [4] and of transition metal dichalcogenides [5,6] gave a powerful impetus to development of optics of low-dimensional structures. One of the important optical methods of investigating two-dimensional materials is the Raman scattering spectroscopy, primarily involving scattering on phonons [7].

For translationally invariant samples, momentum conservation in the sample plane imposes a restriction on the total momentum of excitations emitted or absorbed in the material during Raman scattering in its standard version: since the photon momentum is negligibly small compared to any typical scales in a solid, the total momentum of the excitations may be taken equal to zero. The situation may change significantly when scattering occurs in the presence of a sharp metallic tip that enhances the local field of the photon. If the field varies spatially on near-atomic length scales [8,9], then probing of excitations with substantially non-zero momenta becomes possible, which is of particular importance for scattering on a single optical phonon.

Another advantage of such tip-enhanced Raman scattering (TERS) is the possibility of changing the distance z_T between the tip and the sample within the same experiment, while in the standard version of Raman scattering the only control parameters are the frequencies and the polarizations of the incident and the scattered photons. The measured dependence of the spectrum on the distance z_T [10] obviously contains information about the phonons emitted in the sample. Theoretical studies [11,12] investigated in detail the dependence of TERS spectra on the geometry of experiment (in particular, on the distance z_T), but the question of which phonon-related quantity determined the TERS spectrum, and how to deduce that quantity using the measured dependence of the spectrum on z_T was not fully clarified.

In the present work, an answer to this question is formulated for the case of one-phonon non-resonant Raman scattering. Formally, this answer is expressed by equations (3) and (4) below. The quantity in question turns out to be the phonon spectral function which depends on frequency ω and wave vector $\mathbf{q}$, and includes both dispersion and decay of the phonon. The TERS spectrum is determined by the convolution of this spectral function in $\mathbf{q}$ with a certain integral kernel derived from solution of Maxwell's equations for the specific geometry of experiment and depending on the distance z_T. Knowing the measured spectrum as a function of frequency and distance z_T and assuming the isotropic dependence of the spectral function on $\mathbf{q}$, one may in principle reconstruct the spectral function by deconvolution. The integral kernel is calculated here explicitly for the simplest model geometry where the tip is represented by a polarizable point dipole.

General relations for non-resonant one-phonon scattering

Let us consider a two-dimensional crystal in the $z = 0$ plane. Optical phonons is such crystal may be described by the phononic displacement field operator consisting of a single scalar component $\hat{u}(\mathbf{r}_\parallel)$ for the scalar A_{1g}-phonon or two components $\hat{u}_x(\mathbf{r}_\parallel)$, $\hat{u}_y(\mathbf{r}_\parallel)$ for the degenerate E_{2g}-phonons (for example, in graphene). Here, $\mathbf{r}_\parallel = (x, y)$ denotes coordinates in the crystal plane. Three-dimensional photons are described by the electric field operator $\hat{\mathbf{E}}(\mathbf{r})$, where $\mathbf{r} = (x, y, z)$.

The main contribution to Raman scattering comes from a process where electronic excitations serve as intermediate states [13]. In the case of non-resonant one-phonon scattering where energies of these intermediate states are far from the incident and scattered photon energies, dependence of the photon-photon-phonon vertex on momenta and frequencies may be neglected, so one may work with the effective Hamiltonian describing the local photon-photon-phonon interaction in the long-wavelength approximation,

$$\hat{H}_{\text{int}} = \frac{\Xi_{ij\mu}}{2} \int d^2\mathbf{r}_\parallel \hat{E}_i(\mathbf{r}_\parallel)\hat{E}_j(\mathbf{r}_\parallel, 0)\hat{u}_\mu(\mathbf{r}_\parallel), \tag{1}$$

where $i, j = x, y$ are the Cartesian indices in the plane, and the index μ labels the phonon field components. The form of the tensor $\Xi_{ij\mu} = \Xi_{ji\mu}$ is determined by the crystal geometry: $\Xi_{ij\mu} = \Xi\delta_{ij}$ for the scalar A_{1g}-phonons (for which the index μ is absent), or $\Xi_{xxy} = -\Xi_{yyy} = \Xi_{xyx} = \Xi_{yxx} = \Xi$ for the E_{2g}-phonons (see [14,15] for graphene; here, the component $\hat{u}_x$ is taken with the opposite sign). The effective dimensionless coupling constant Ξ may have a smooth dependence on the incident photon frequency and electronic doping level. It can be related to an observable quantity — free-space Raman scattering efficiency η, i.e. the absolute probability, for normally incident photon with a given linear polarization and frequency $\omega_{\text{i}} = ck_{\text{i}}$, of being scattered into the full solid angle 4π with any polarization. Specifically, the Fermi golden rule in the lowest-order perturbation theory with respect to Hamiltonian (1) for the scalar phonons A_g gives

$$\eta = \frac{4\pi\Xi^2}{3} \frac{\hbar\omega_{\text{i}}^2(\omega_{\text{i}} - \omega_{\text{ph}})^2}{\rho_0\omega_{\text{ph}}c^4}, \tag{2}$$

where ρ_0 denotes the mass density of the crystal. For the doubly degenerate E_{2g}-phonons, the expression is the same, but with an additional factor of 2.

We will assume that the crystal is excited by a classical monochromatic external field with frequency $\omega_{\text{i}} > 0$, which may be represented by a shift of the electric field operator, $\hat{E}_i(\mathbf{r}) \to \hat{E}_j(\mathbf{r}) + \mathscr{E}_j(\mathbf{r})e^{-i\omega_{\text{i}}t} + \mathscr{E}_j^*(\mathbf{r})e^{i\omega_{\text{i}}t}$, in Hamiltonian (1). The spatial profile of the excitation field $\mathscr{E}_j(\mathbf{r})$ should be found from the solution of Maxwell's equations in the given geometry and in the presence of the tip. Intensity of the scattered signal at frequency $\omega_{\text{s}} > 0$ measured in an arbitrary point $\mathbf{r}_0$ is proportional to the electric field correlator [16],

$$S(\mathbf{r}, \omega_{\text{s}}) = \lim_{T\to\infty} \int_{-T}^{T} \frac{dt}{2T} \int_{-\infty}^{\infty} d\tau\, e^{i\omega_{\text{s}}\tau} \langle \hat{\mathbf{E}}(\mathbf{r}, t)\hat{\mathbf{E}}(\mathbf{r}, t + \tau)\rangle, \tag{3}$$

where the field operators are taken in the Heisenberg representation including the interaction with phonons and with the external oscillating field (the latter formally necessitates time averaging because the correlator may depend not only on the time difference). If detection is performed upon focusing by a lens, then instead of the field in a given point, an integral over the corresponding solid angle should appear.

Expansion of the evolution operator in the interaction representation up to the second order in the coupling constant Ξ and in the pumping field gives the following expression for the electric field correlator entering the expression for the detected signal [3] (taken in different spatial points for greater generality):

$$\lim_{T\to\infty} \int_{-T}^{T} \frac{dt}{2T} \int_{-\infty}^{\infty} d\tau\, e^{i\omega_{\text{s}}\tau} \langle \hat{E}_{j1}(\mathbf{r}_1, t)\hat{E}_{j2}(\mathbf{r}_2, t + \tau)\rangle$$

$$= \Xi_{ij\mu}\Xi_{i'j'\mu'} \int d^2\mathbf{r}_\parallel d^2\mathbf{r}'_\parallel G^R_{j_2 j}(\mathbf{r}_2, \mathbf{r}_\parallel, \omega_{\text{s}})\mathscr{E}_i\mathbf{r}_\parallel)$$

$$\times\, i\hbar D^<_{\mu\mu'}(\mathbf{r}_\parallel - \mathbf{r}'_\parallel, \omega_{\text{s}} - \omega_{\text{i}})\mathscr{E}^*_{i'}(\mathbf{r}'_\parallel)G^A_{j'j_1}(\mathbf{r}'_\parallel, \mathbf{r}_1, \omega_{\text{s}}), \tag{4}$$

where convolution with respect to all repeated indices is implied. The Green's functions of photons (G) and phonons (D) are defined below.

The retarded photonic Green's function $G^R_{ij}(\mathbf{r}, \mathbf{r}', \omega)$ defines the electric field response to an external three-dimensional polarization $\mathbf{P}^{\text{ext}}(\mathbf{r}', t')$ oscillating at frequency ω without accounting for the interaction (1), but accounting for the whole dielectric/metallic environment, including the tip. Assuming that this environment is fully defined by the local dielectric function $\varepsilon(\mathbf{r}, \omega)$, the retarded Green's function can be found from Maxwell's equations,

$$\left[\varepsilon(\mathbf{r}, \omega)\frac{\omega^2}{c^2} - \boldsymbol{\nabla} \times \boldsymbol{\nabla}\times\right] \mathbf{E}(\mathbf{r}, \omega) = -4\pi\frac{\omega^2}{c^2}\mathbf{P}^{\text{ext}}(\mathbf{r}, \omega), \tag{5a}$$

$$E_i(\mathbf{r}, \omega) = -\int d^3\mathbf{r}' G^R_{ij}(\mathbf{r}, \mathbf{r}', \omega)\, P^{\text{ext}}_j(\mathbf{r}', \omega), \tag{5b}$$

i.e. $G^R_{ij}(\mathbf{r}, \mathbf{r}', \omega)$ (up to a factor) is an operator inverse to the differential operator on the left-hand side of equation (5a) with boundary conditions corresponding to outgoing waves. The advanced Green's function $G^A_{ij}(\mathbf{r}, \mathbf{r}', \omega) = [G^R_{ji}(\mathbf{r}', \mathbf{r}, \omega)]^*$.

The phonon Green's function $D^<_{\mu\mu'}(\mathbf{r}_\parallel, \omega)$ (correlator of the phonon displacements) entering expression (4), is related to the phonon spectral function or the imaginary part of the advanced Green's function $D^A_{\mu\mu'}(\mathbf{q}, \omega)$ in the momentum representation,

$$i\hbar D^<_{\mu\mu'}(\mathbf{r}_\parallel, \omega) = \int \frac{d^2\mathbf{q}}{(2\pi)^2} e^{i\mathbf{q}\mathbf{r}_\parallel} \frac{2\hbar \operatorname{Im} D^A_{\mu\mu'}(\mathbf{q}, \omega)}{e^{\hbar\omega/T} - 1}, \tag{6}$$

where T is the crystal temperature. For example, for the scalar phonons with dispersion $\omega_{\mathbf{q}}$ and amplitude decay γ, the advanced Green's function is given by

$$D^A(\mathbf{q}, \omega) = \frac{1/\rho_0}{\omega^2 - 2i\omega\gamma - \omega^2_{\mathbf{q}}}. \tag{7}$$

For the degenerate E_{2g}-phonons, longitudinal and transverse modes have different dispersion and decay. The key result contained in equation (4) is the following: all information about phonons that can be deduced from the non-resonant Raman scattering spectrum is contained in the phonon spectral function $\mathrm{Im}D^A_{\mu\mu'}(\mathbf{q},\omega)$. The Bose–Einstein distribution included in equation (6) implies only that a non-zero phonon population is necessary for the anti-Stokes scattering ($\omega_\mathrm{s} > \omega_\mathrm{i}$), while for the Stokes scattering ($\omega_\mathrm{s} < \omega_\mathrm{i}$), $D^<(\omega < 0)$ is non-zero even at zero temperature, which corresponds to phonon emission into the crystal.

Equations (3) and (4) are the main result of this work. They admit a simple physical interpretation. The field at the point $\mathbf{r}_0$, whose intensity is included in equation (3), is induced by polarization in the sample. The photon Green's function G^R (or G^A) gives the contribution to the field induced by polarization at the point $\mathbf{r}_\parallel$ (or contribution to the complex-conjugate field induced by polarization at the point $\mathbf{r}'_\parallel$). The polarization in the sample induced by the excitation field $\mathscr{E}$ is proportional to the phononic displacement. The correlator of these displacements (the phonon Green's function $D^<$), thus, defines the correlator of the induced polarization in different points.

As far as the photonic part is concerned, equations (3) and (4) are equivalent to equation (6) of Ref. [11] (up to the factor $4\pi\omega^2/c^2$ in the photon Green's function definition, arising from the right-hand side of equation (5a)). However, equation (6) [11] contains a phenomenologically introduced object (polarizability correlator) whose relation with the phonon properties of the sample was not traced down. Here, this object is explicitly identified with the phonon Green's function. It is also obvious that such identification is essentially based on the assumption of locality of the effective photon-phonon interaction (1). In case of resonant scattering, propagation of virtual electron-hole pairs that serve as intermediate states for the Raman scattering breaks this locality [14,17] leading to a more complex relation between the Raman spectrum and the sample properties. Investigation of this more complex case in beyond the scope of the present study.

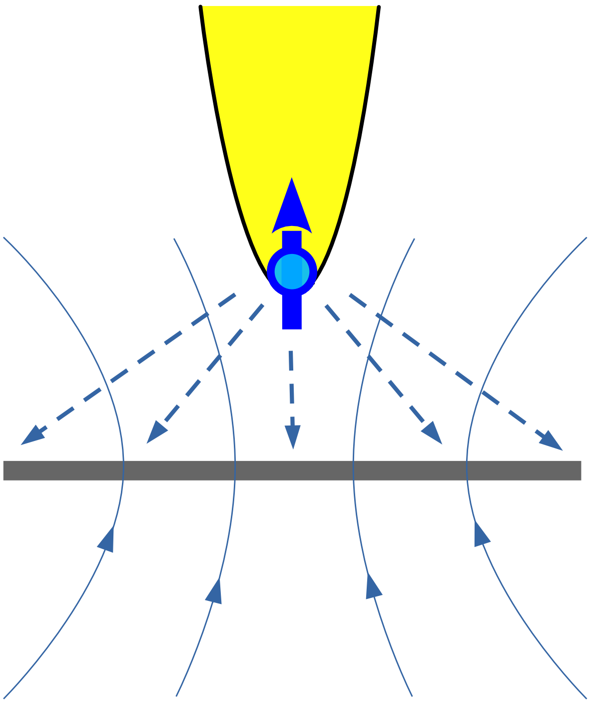

Figure 1. A sketch of the two-dimensional sample, sharp tip, focused excitation light beam (solid lines), induced dipole at the end of the tip, and light incident from the tip to the sample (dashed lines).

Explicit calculation using the simplest model of the tip

According to equation (4), the possibility of probing the spectral function $\mathrm{Im}D^A_{\mu\mu'}(\mathbf{q},\omega)$ at finite wave vectors $\mathbf{q}$ (which would allow measurement of phonon dispersion and decay) is defined by the spatial dependence of the excitation field and phonon Green's functions in the presence of the tip. Let us determine this dependence for an axially symmetric experimental geometry, while modelling the tip as a point dipole with a given polarizability, placed at the point $\mathbf{r}_\mathrm{T} = (0,0,z_\mathrm{T})$ (the z axis coincides with the symmetry axis, the sample is placed in the $z = 0$ plane). The distance $z_\mathrm{T} \sim 1 - 10\,\mathrm{nm}$ is assumed much smaller than the wavelength of light λ. For the axially symmetric tip, the polarizability tensor $\alpha_{ij}(\omega)$ has only two independent components: $\alpha_{xx}(\omega) = \alpha_{yy}(\omega) \equiv \alpha_\parallel(\omega)$ and $\alpha_{zz}(\omega)$.

For excitation by a radially polarized focused light beam (as in experiments [10,18]), the component of the beam's electric field in the plane of the two-dimensional crystal vanishes strictly on the axis and grows slowly (at distances of about λ) away from the axis. Consequently, the main part of polarization induced directly by the focused beam field is far from the tip and the scattered signal generated by this polarization is insensitive to the tip position. At the same time, the perpendicular component $\mathscr{E}_z$ of the focused beam field is not small near the axis; though this component does not act on the sample (Hamiltonian (1) contains only the in-plane field), it induces a dipole moment in the tip, and this dipole induces a field in the sample plane (Figure 1). This field induces polarization in the sample in the vicinity of the tip. Thus, the field of the excitation beam itself (S- and TS-contributions according to [11]) can be neglected, and the excitation field $\mathscr{E}_j(\mathbf{r}_\parallel)$ can be taken as the field of a point dipole $\alpha_{zz}(\omega_\mathrm{i})\mathscr{E}_{0z}$ oscillating with frequency ω_i perpendicularly to the crystal plane at distance z_T above the crystal:

$$\mathscr{E}_j(\mathbf{r}_\parallel) = -\alpha_{zz}(\omega_\mathrm{i})\mathscr{E}_{0z}\frac{3z_\mathrm{T}x_{\parallel j}}{(r_\parallel^2 + z_\mathrm{T}^2)^{5/2}}. \qquad (8)$$

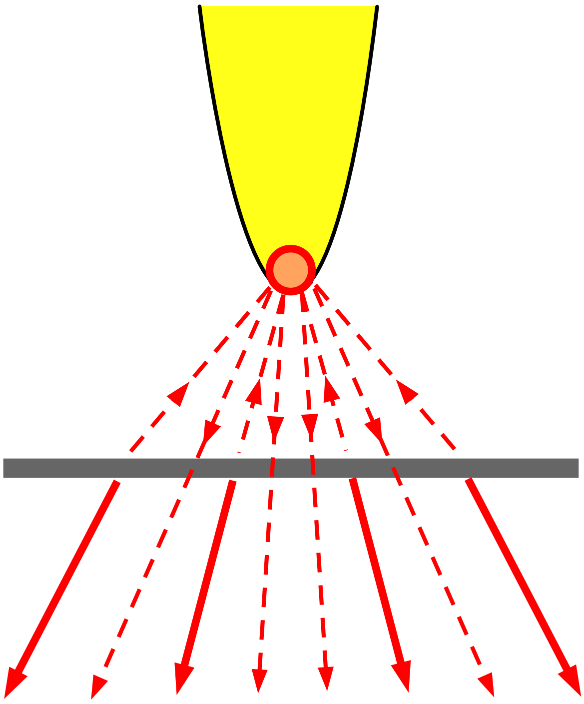

Figure 2. A sketch of the two-dimensional sample, sharp tip, light propagating from the sample directly to the detector (solid lines) and light going to the detector after scattering on the tip (dashed lines).

To account for the tip in the photon Green's function, it should be noted that the far field is produced both directly by the polarization in the sample (oscillating at frequency ω_s), as well as by the tip where charges are induced by the near field from the polarization in the sample (Figure 2). Since scattered light is detected at distances that are at least of the order of the wavelength of light, i.e. much longer than the typical size of the tip and of the sample area affected by the tip, the far field is determined by the total dipole moment of the sample and the tip. Thus, if the photon Green's function without the tip is denoted by $\bar{G}^R_{ij}(\mathbf{r}, \mathbf{r}', \omega)$, then one can approximately write

$$G^R_{j_2 j}(\mathbf{r}_0, \mathbf{r}_\parallel, \omega_\mathrm{s}) = \bar{G}^R_{j_2 j_3}(\mathbf{r}_0, 0, \omega_\mathrm{s}) \times \left[\delta_{j_3 j} - \alpha_{j_3 j_4}(\omega_\mathrm{s}) \bar{G}^R_{j_4 j}(\mathbf{r}_\mathrm{T}, \mathbf{r}_\parallel, \omega_\mathrm{s})\right]. \tag{9}$$

If the scattered light is focused by a lens at some spatial point $\mathbf{r}_0 = (0, 0, z_0)$ where the detector is placed, then the tensor structure of the first factor in this expression is simplified due to the axial symmetry:

$$\bar{G}^R_{xx}(\mathbf{r}_0, 0, \omega_\mathrm{s}) = \bar{G}^R_{yy}(\mathbf{r}_0, 0, \omega_\mathrm{s}) \equiv g_\parallel,$$

$$\bar{G}^R_{zz}(\mathbf{r}_0, 0, \omega_\mathrm{s}) \equiv g_z.$$

In this case, the whole detection scheme is characterized by two constants $g_\parallel$ and g_z. In the second factor in equation (9) in $\bar{G}^R_{j_4 j}(\mathbf{r}_\mathrm{T}, \mathbf{r}_\parallel, \omega_\mathrm{s})$ one may neglect retardation (i.e. take it in the static dipole-dipole approximation). Then, expression (9) takes the form (where $x_{\parallel j_2}, x_{\parallel j}$ are components of $\mathbf{r}_\parallel$ in the crystal plane, while the z-component is treated separately):

$$G^R_{j_2 j}(\mathbf{r}_0, \mathbf{r}_\parallel, \omega_\mathrm{s}) = g_\parallel \delta_{j_2 j}\left[1 - \frac{\alpha_\parallel(\omega_\mathrm{s})}{(r_\parallel^2 + z_\mathrm{T}^2)^{3/2}}\right] + 3g_\parallel \frac{\alpha_\parallel(\omega_\mathrm{s}) x_{\parallel j_2} x_{\parallel j}}{(r_\parallel^2 + z_\mathrm{T}^2)^{5/2}}, \quad j_2, j = x, y \tag{10a}$$

$$G^R_{zj}(\mathbf{r}_0, \mathbf{r}_\parallel, \omega_\mathrm{s}) = -3g_z \frac{\alpha_{zz}(\omega_\mathrm{s}) z_\mathrm{T} x_{\parallel j}}{(r_\parallel^2 + z_\mathrm{T}^2)^{5/2}}. \tag{10b}$$

By substituting these expressions into general equations (3) and (4), we obtain an explicit result for the scalar phonon case:

$$S(\mathbf{r}_0, \omega_\mathrm{s}) = |2\pi\alpha_{zz}(\omega_\mathrm{i})\mathscr{E}_{0z}|^2 \Xi^2 \times \int \frac{d^2\mathbf{q}}{(2\pi)^2} i\hbar D^<(\mathbf{q}, \omega_\mathrm{s} - \omega_\mathrm{i}) \times \left[|g_\parallel|^2 \left| q e^{-q z_\mathrm{T}} + \frac{3\alpha_\parallel(\omega_\mathrm{s})}{z_\mathrm{T}^3} \frac{2\mathscr{J}_{3,1}(q z_\mathrm{T}) - \mathscr{J}_{1,1}(q z_\mathrm{T})}{z_\mathrm{T}} \right|^2 + |g_z|^2 \left| \frac{3\alpha_{zz}(\omega_\mathrm{s})}{z_\mathrm{T}^3} \frac{3\mathscr{J}_{2,0}(q z_\mathrm{T})}{z_\mathrm{T}} \right|^2 \right] \tag{11}$$

Here, integrals of the Bessel functions $J_n(z)$ are introduced:

$$\mathscr{J}_{l,n}(q z_\mathrm{T}) \equiv \int\limits_0^\infty \frac{\xi^{l+1} d\xi}{(\xi^2 + 1)^5} J_n(q z_\mathrm{T} \xi), \tag{12}$$

some of which may be expressed in terms of the modified Bessel functions: $\mathscr{J}_{n,n}(q z_\mathrm{T}) = (q z_\mathrm{T})^4 K_{4-n}(q z_\mathrm{T})/384$.

For the doubly degenerate E_{2g}-phonons, the calculation can be done in the isotropic approximation, valid for sufficiently small wave vectors (when, in fact, the effective Hamiltonian (1) is only applicable). Then the phonon Green's function has an explicit tensor structure expressed in terms of the longitudinal (L) and transverse (T) components:

$$D_{\mu\mu'}(\mathbf{q}, \omega) = \frac{q_\mu q_{\mu'}}{q^2} D_L(q, \omega) + \left(\delta_{\mu\mu'} - \frac{q_\mu q_{\mu'}}{q^2}\right) D_T(q, \omega). \tag{13}$$

In this approximation, we obtain

$$S(\mathbf{r}_0, \omega_\mathrm{s}) = |2\pi\alpha_{zz}(\omega_\mathrm{i})\mathscr{E}_{0z}|^2\Xi^2 \int \frac{d^2\mathbf{q}}{(2\pi)^2}$$

$$\times \left[i\hbar D_L^<(\mathbf{q}, \omega_\mathrm{s} - \omega_\mathrm{i}) + i\hbar D_T^<(\mathbf{q}, \omega_\mathrm{s} - \omega_\mathrm{i})\right]$$

$$\times \left[|g_\parallel|^2 \left| q e^{-qz_\mathrm{T}} + \frac{3\alpha_\parallel(\omega_\mathrm{s})}{z_\mathrm{T}^3} \frac{\mathscr{J}_{3,1}(qz_\mathrm{T}) - 2\mathscr{J}_{1,1}(qz_\mathrm{T})}{2z_\mathrm{T}} \right|^2\right.$$

$$+ |g_\parallel|^2 \left| \frac{3\alpha_\parallel(\omega_\mathrm{s})}{z_\mathrm{T}^3} \frac{3\mathscr{J}_{3,3}(qz_\mathrm{T})}{2z_\mathrm{T}} \right|^2$$

$$\left. + \frac{|g_z|^2}{2} \left| \frac{3\alpha_{zz}(\omega_\mathrm{s})}{z_\mathrm{T}^3} \frac{3\mathscr{J}_{2,2}(qz_\mathrm{T})}{z_\mathrm{T}} \right|^2 \right]. \tag{14}$$

Qualitative discussion

The point dipole approximation used for the tip is valid only at distances z_T that are much longer than the typical tip size R_T. Since for a metal tip without resonances the polarizability $\alpha_{ij}(\omega) \sim R_\mathrm{T}^3$, the cumbersome terms with integrals $\mathscr{J}_{l,n}(qz_\mathrm{T})$ proportional to α/z_T^3 are beyond the scope of the approximation and may be discarded. In this case, the integral kernel takes a very simple form $\propto q^2 e^{-2qz_\mathrm{T}}$. However, if the scattered photon frequency falls near a plasmon resonance in the tip, then a situation with $\alpha \gg R_\mathrm{T}^3$ is possible; then all terms in expressions (11) and (14) become important.

In typical experiments, z_T can be generally made approximately equal to or even smaller than the typical tip size R_T, so to describe such situation realistically, it is necessary to go beyond the dipole approximation for the tip. However, two other approximations used above (axially symmetric geometry of experiment and smallness of the tip size compared to the wavelength of light) remain quite realistic. In this case, to generalize the above calculation, it is necessary to solve numerically the Poisson equation in the specified dielectric structure (substrate, tip) at each value of z_T. As a result, three scalar functions of the radial coordinate $r_\parallel$ should be calculated. First, one should find the radial electric field produced by charges which are induced in the tip by a homogeneous external field along the z axis, to use it instead of Eq. (8). Second, to generalize Eqs. (10), one should find the radial and the axial components of the tip's dipole moment induced by the field of a point charge placed at a point $(r_\parallel, 0, 0)$. As a result, the integral kernel, to be convoluted with the phonon Green's function, will be determined by one-dimensional integrals of these functions and their derivatives with respect to $r_\parallel$ with Bessel functions. Such calculation would be justified for modeling a particular experiment and, thus, goes beyond the scope of the present study.

Nevertheless, the obtained results give an insight into the qualitative picture. In the realistic case, the integral kernel should have a smooth wave-vector dependence on the typical scale $q \sim \min\{1/z_\mathrm{T}, 1/R_\mathrm{T}\}$. Thus, measuring the dependence of the signal on z_T enables one to probe the phonon spectral function on the scale $q \lesssim 1/R_\mathrm{T}$. Note that, if the dependence of this spectral function on q at this frequency has some fine structure on scales smaller than q itself (for example, has a narrow peak at some finite value of q defined by the phonon dispersion, with a width defined by weak phonon decay), then it might be difficult to reconstruct this fine structure from the dependence of the signal on z_T.

Conclusion

Dependence of the TERS spectrum on the tip position is determined by two main factors: the photonic factor depending on the electric field configuration in the whole structure (incident field, sample, tip and detector) and the factor describing excitations in the sample and interaction between these excitations and field. The photonic factor is determined from the solution of Maxwell's equations in the given structure and was studied in detail for two-dimensional materials in [11,12]. As for the sample whose excitations at final wave vectors become available for probing due to the tip's near field, the situation is more complicated. The corresponding factor obviously depends on the type of excitations, their dynamics, and their interaction with light.

The present study investigated the one-phonon nonresonant Raman scattering on long-wavelength phonons in two-dimensional materials when the interaction between a phonon and photon may be taken as local and instantaneous (in other words, dependence of the corresponding vertex on momenta and frequencies may be neglected). It is shown that the sample factor defining the TERS signal at a given frequency reduces to the spectral function of the emitted phonon. Its convolution in momentum with the photonic factor gives the TERS signal at each frequency. Thus, when the photonic factor for each of the tip positions is known, information about the phonon spectral function may be in principle extracted by deconvolution. For resonant scattering, the assumption about locality of the effective interaction may be substantially violated, therefore this case requires a separate study.

The corresponding factors were calculated explicitly for the simplest model geometry where the whole structure is axially symmetric and small compared with the wavelength of light, and the tip is represented by a polarizable point dipole. It is necessary to go beyond this latter approximation in order to describe experiments realistically (because the distance between the tip and sample may be quite comparable with the typical tip size), and the Poisson equation should be solved numerically in a dielectric structure corresponding to each given experiment. It may be also useful to address a more general geometry (various detector positions relative to the tip, light polarization measurements) to obtain additional information about the sample (for example, about the tensor structure of the photon-phonon interaction), but it would require more cumbersome calculations.

Acknowledgments

The author is greatly indebted to V.M. Agranovich for supervision and support at the early stages of the author's research career, and for the priceless knowledge in the theory of optical properties of solids and nanostructures.

The author is also grateful to L.G. Cançado, R. Corrêa, A. Jorio and R.B. Nadas for many discussions that stimulated the author's interest in the subject of the present work.

Conflict of interest

The author declares that he has no conflict of interest.

References

[1] V.M. Agranovich, O.A. Dubovsky. JETP Letters, **3**, 345 (1966).
[2] V.M. Agranovich, *Excitations in Organic Solids* (Oxford University Press, Oxford, 2009).
[3] E.I. Ivchenko. *Optical Spectroscopy of Semiconductor Nanostrucutures* (Alpha Science International, Harrow, 2005).
[4] K.S. Novoselov, A.K. Geim, S.V. Morozov, D. Jiang, Y. Zhang, S.V. Dubonos, I.V. Grigorieva, A.A. Firsov. Science **306**, 666 (2004). DOI: 10.1126/science.1102896
[5] A. Splendiani, L. Sun, Y. Zhang, T. Li, J. Kim, C.-Y. Chim, G. Galli, F. Wang. Nano Lett., **10**, 271 (2010). DOI: 10.1021/nl903868w
[6] K.F. Mak, C. Lee, J. Hone, J. Shan, T.F. Heinz, Phys. Rev. Lett. **105**, 136805 (2010). DOI: 10.1103/PhysRevLett.105.136805
[7] A.C. Ferrari, D.M. Basko. Nature Nanotechnology, **8**, 235 (2013). DOI: 10.1038/NNANO.2013.46
[8] R. Zhang, Y. Zhang, Z.C. Dong, S. Jiang, C. Zhang, L.G. Chen, L. Zhang, Y. Liao, J. Aizpurua, Y. Luo, J.L. Yang, J.G. Hou. Nature, **498**, 82 (2013). DOI: 10.1038/nature12151
[9] J. Lee, K.T. Crampton, N. Tallarida, V.A. Apkarian. Nature, **568**, 78 (2019). DOI: 10.1038/s41586-019-1059-9
[10] R.B. Nadas, A.C. Gadelha, T.C. Barbosa, C. Rabelo, T. de Lourenço e Vasconcelos, V. Monken, A.V.R. Portes, K. Watanabe, T. Taniguchi, J.C. Ramirez, L.C. Campos, R. Saito, L.G. Cançado, A. Jorio. Nano Lett. **23**, 8827 (2023). DOI: 10.1021/acs.nanolett.3c00851
[11] L.G. Cançado, R. Beams, A. Jorio, L. Novotny. Phys. Rev. X, **4**, 031054 (2014). DOI: 10.1103/PhysRevX.4.031054
[12] B.C. Publio, B.S. Oliveira, C. Rabelo, H. Miranda, T.L. Vasconcelos, A. Jorio, L.G. Cançado. Phys. Rev. B **105**, 235414 (2022). DOI: 10.1103/PhysRevB.105.235414
[13] Max Born and Kun Huang. *Dynamical Theory of Crystal Lattices* (Oxford University Press, 1954).
[14] D.M. Basko. Phys. Rev. B, bf78, 125418 (2008). DOI: 10.1103/PhysRevB.78.125418
[15] D.M. Basko. Phys. Rev. B, **79**, 129902(E) (2009). DOI: 10.1103/PhysRevB.79.129902
[16] R.J. Glauber. Phys. Rev., **130**, 2529 (1963).
[17] D.M. Basko. Phys. Rev. B, **79**, 205428 (2009). DOI: 10.1103/PhysRevB.79.205428
[18] H. Miranda, V. Monken, J.L.E. Campos, T.L. Vasconcelos, C. Rabelo, B.S. Archanjo, C.M. Almeida, S. Grieger, C. Backes, A. Jorio, L.G. Cançado. 2D Mater. **10**, 015002 (2023). DOI: 10.1088/2053-1583/ac988f

Translated by E.Ilinskaya